

Identification of Putative Peroxide Intermediates of Peroxidases by Electronic Structure and Spectra Calculations

Danni L. Harris* and Gilda H. Loew

Contribution from the Molecular Research Institute, Palo Alto, California 94304

Received May 21, 1996. Revised Manuscript Received August 19, 1996[⊗]

Abstract: The INDO/ROHF/CI quantum chemical method has been used to calculate the electronic structure and spectra of two candidate peroxide intermediates of model peroxidases. In the enzymatic cycle of this family of oxidative metabolizing heme proteins, hydrogen peroxide is required to transform the ferric resting state to the catalytically active, ferryl Fe=O, compound **I** species. While a peroxide complex has been proposed as a key intermediate in this reaction, this intermediate species is too transient to have thus far been definitively characterized. Electronic spectra observed prior to compound **I** formation during the reaction of H₂O₂ with both wild type and the R38L mutant of horseradish peroxidase C (HRP-C) have been attributed to this intermediate. There are, however, significant qualitative differences in these spectra in the 300–450-nm region, with a “hyper-Soret” observed in one and a normal Soret, not very different from the resting state, found in the other. In the absence of any additional information, it is not possible from these reported spectra alone to identify the species that give rise to them or to understand these differences. In order to identify the origin of these spectra and their differences, we have calculated the electronic structure and spectra of two possible forms of the peroxide intermediate of model peroxidases, one with a neutral peroxide and the other with an anionic form (OOH[−]) as the heme Fe ligand. Formation of the anion is possible by proton transfer to a nearby histidine residue, already implicated in compound **I** formation. A comparison of the calculated spectra for these two transient species indicates them to be quite distinct. Comparisons of the two spectra with those experimentally observed suggest that the “hyper-porphyrin” spectrum observed in the wild type (WT) HRP-C experiments originates from the OOH[−] form of this transient intermediate in a low-spin ground state, while the normal Soret observed in the R38L HRP-C mutant experiment originates from the neutral peroxide form in a high-spin ground state. Thus by relating species to spectra, and by examining the consistency of calculated and observed spectra, a plausible identification has been made of the transient intermediate species in the pathway from the resting state to compound **I** of peroxidases.

Introduction

Peroxidases are ubiquitous oxidative metabolizing heme proteins widely distributed in plants, fungal, and bacteria and also found in mammalian species. They are among the most extensively studied enzymes with a long history of mechanistic and spectroscopic investigations. It is now firmly established from these studies that, as shown schematically in Figure 1, the common feature of all peroxide oxidations¹ is the requirement of stoichiometric amounts of peroxide that transform the ferric heme resting state, via a putative peroxide intermediate, to the catalytically active compound **I**, Fe=O ferryl species, two oxidation states above the resting state. It is this form of the enzyme that initiates two sequential one-electron oxidations of a variety of organic substrates such as phenols and aromatic amines, via a second intermediate, compound **II**, returning to its ferric resting state.

Both compounds **I** and **II** are stable enough to have been characterized by a variety of spectroscopic methods² and a recent crystal structure of a compound **I** species definitely confirmed the Fe=O nature of this intermediate.^{3,4} Characterization of the transient peroxide intermediate and mechanistic elucidation

of the pathway to formation of compound **I** from it has proven more elusive. These features are currently among the major unresolved aspects of peroxidase function.

A proposed mechanism of compound **I** formation based on the first known peroxidase structure cytochrome *c* peroxidase (CCP) is shown in Figure 1. In this mechanism, (a) peroxide binds directly to the heme iron, (b) a nearby histidine abstracts a proton from the proximal oxygen, forming a peroxyanion species, (c) the distal oxygen of this species is then protonated by the imidazole, thus (d) resulting in facile cleavage of the O–O bond and formation of compound **I** and water with this leaving group stabilized by electrostatic interactions with a nearby arginine residue.

In past studies,⁵ we examined the nature of the putative peroxide intermediate of CCP by molecular dynamic simulations using the known crystal structure of CCP.⁶ The results indicated the formation of a stable CCP–HOOH complex, with the peroxide binding to the Fe as a ligand in a bent, end-on geometry, rather than a bridged structure. In addition, during the MD simulations at 300 K, a rapid exchange of oxygen atoms as ligands of the heme iron was observed, with equal probability of each oxygen serving as a ligand, indicative of a low-energy barrier between them.

The dynamic behavior found provided direct support for the proposed mechanism of compound **I** formation and the role of His and Arg in it. Specifically, the peroxide hydrogens were

[⊗] Abstract published in *Advance ACS Abstracts*, October 1, 1996.

(1) Frew, J. E.; Jones, P. *Adv. Inorg. Bioinorg. Mech.* **1984**, *3*, 175–212.

(2) Dunford, H. B. Horseradish peroxidase: structure and kinetic properties. In *Peroxidases in Chemistry and Biology*; Vol. 2. Everse, J.; Everse, K.; Grisham, M. B.; Eds.; CRC Press: Boca Raton, FL, 1991; pp 1–24.

(3) Edwards, S. L.; Nguyen, H. X.; Hamlin, R. C.; Kraut, J. *Biochemistry* **1987**, *26*, 1503–1511.

(4) Fulop, V.; Phizackerley, R. P.; Aoltis, S. M.; Clifton, I. J.; Wakatsuki, S.; Erman, J.; Hadju, J.; Edwards, S. L. *Structure* **1994**, *2*, 201–208.

(5) Collins, J. R.; Du, P.; Loew, G. H. *Biochemistry* **1992**, *31*, 11166–11174.

(6) Finzel, B. C.; Poulos, T. L.; Kraut, J. *J. Biol. Chem.* **1984**, *259*, 13027–13036.

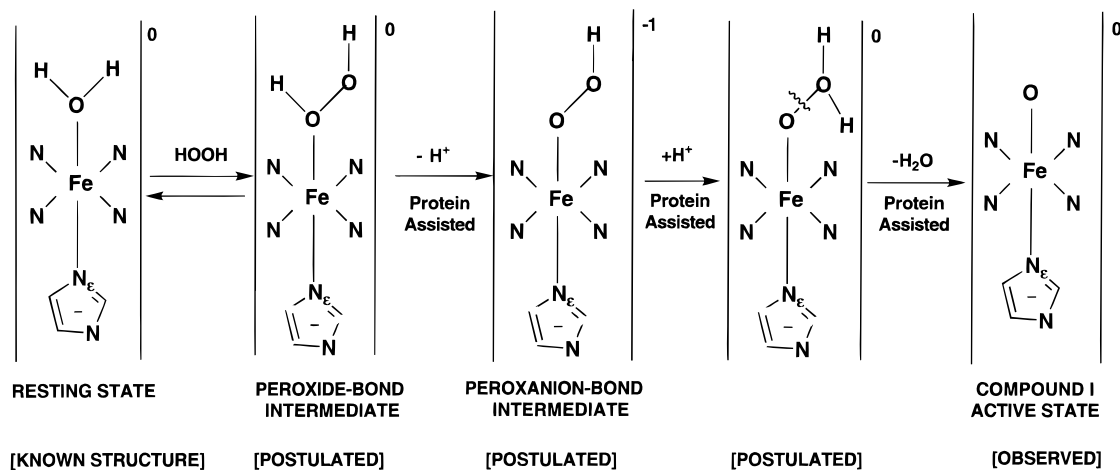


Figure 1. Proposed steps in formation of the catalytically active oxidizing species from the resting state of peroxidases.

found to form hydrogen bonds with the N_{ϵ} of the histidine. As the O atoms of the peroxide alternate as ligands to the iron, the H atoms alternate as partners with the imidazole nitrogen of this proximal histidine. This behavior is consistent with the proposed role of this His residue as an acid–base catalyst by abstracting a proton from the proximal oxygen and transferring it to the distal peroxide oxygen, facilitating O–O bond cleavage. The results also confirmed a role for the nearby Arg in electrostatic stabilization of this leaving group since the distal peroxide oxygen remains near the cationic Arg $H-N_{\epsilon}$ during the simulation.

Investigations of the existence of a transient peroxide species by spectroscopic methods have also been made.^{7–10} In these rapid scan spectroscopic studies of the reaction of peroxide with peroxidase, changes were monitored primarily in the Soret bands, intense absorptions in the 400-nm region common to all heme spectra. In these studies, it was shown that formation of compound **I** is preceded by a new intermediate of unknown structure in WT HRP,⁷ in mutant R38L HRP,¹⁰ and in a water soluble ferric heme model for the peroxidases, *N*-acetylmicroperoxidase-8 (Ac-MP-8).⁹

In two of these studies, for WT HRP and the water soluble peroxidase model, a dramatic difference was found between the resting state spectrum with a typical Soret at 400 nm and the spectrum attributed to this transient intermediate. The transient spectra reported had the surprising features of a “hyperporphyrin” spectra, or a “split Soret”, with two intense transitions at 330 and 400 nm. Although such spectra have been observed for the related family of oxidizing heme proteins, the cytochrome P450s, this is the first time such spectra have been reported for a peroxidase.

Enigmatically, this additional peak is missing in a rapid scan stopped flow optical spectra of the reaction of a mutant (R38L) HRP-C with H_2O_2 that also indicates the formation of a transient species followed by its conversion to compound **I**. In this latter study, the resting state and putative peroxide complex were reported to have essentially identical spectra in the region 320–450 nm with no sign of the additional peak at 330 nm. It is unlikely that the mutation, although it slows the rate of compound **I** formation, could directly account for the qualitative difference in these spectra, namely the presence in one case

and the absence in the other of an intense additional peak at 330 nm. It is, however, possible that the mutation results in a somewhat different form of the transient intermediate.

Taken together the spectra obtained provide additional evidence for the formation of at least one transient intermediate in the pathway from the resting state to compound **I** of peroxidases. They cannot by themselves, however, lead to the identification of the intermediate or address the origin of the differences obtained in the two spectra.

In the work reported here, we have probed the identity of the putative transient peroxide species, whose spectra have been reported, using quantum chemistry. These methods are ideally suited to help identify the species that are responsible for the observed spectra and to help understand the origin of the differences between them. We have calculated the electronic structure and spectra of the resting state and two plausible candidates for the transient peroxide species, one with a neutral $HOOH$ and the other with an anionic OOH^- ligand, resulting from proton transfer from the peroxide to the imidazole of this histidine that has mechanistic importance in compound **I** formation (Figure 1). It is possible that both the neutral and anionic forms of the transient peroxide peroxidase species could be observed in the pathway from the resting state to compound **I** that was monitored in the experimental rapid scan stopped flow spectra reported.

These calculations were performed using an INDO/S restricted open shell Hartree–Fock configuration interaction (INDO/S-ROHF/CI) method.^{11,12} We have successfully used it in the past to calculate the electronic structure and spectra of many model heme proteins, including myoglobin, peroxidases, catalases, and the cytochrome P450s in a variety of spin, oxidation, and liganded states.^{13–15}

The computations reported here for the two transient model peroxidase peroxide species led to the identification of the putative transient species that are the origin of the observed spectra. They were also used to assign the specific electronic excitations that give rise to each of the spectral lines. The ability to make these assignments of the spectral lines is an additional strength of the computed spectrum, not possible to deduce from the experimental spectrum.

(7) Baek, H. K.; Van Wart, H. E. *Biochemistry* **1989**, *28*, 5714–5719.

(8) Baek, H. K.; Van Wart, H. E. *J. Am. Chem. Soc.* **1992**, *114*, 718–725.

(9) Wang, J.-S.; Baek, H. K.; Van Wart, H. E. *Biochem. Biophys. Res. Instit.* **1991**, *179*, 1320–1324.

(10) Neptuno, J.; Rodriguez-Lopez, J. N.; Smith, A. T.; Thornsley, R. N. T. *J. Biol. Chem.* **1996**, *271*, 4023–4030.

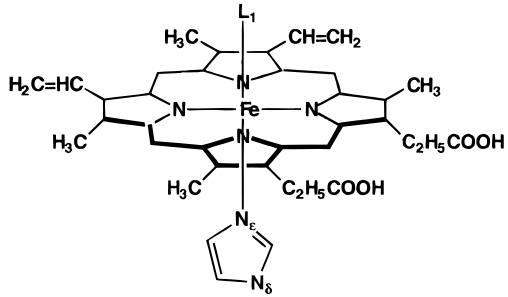
(11) Bacon, A. D.; Zerner, M. C. *Theor. Chim. Acta* **1979**, *53*, 21–54.

(12) Edwards, W. D.; Zerner, M. C. *Theor. Chim. Acta* **1987**, *72*, 347–361.

(13) Du, Ping; Loew, G. H. *Biophys. J.* **1995**, *68*, 69–80.

(14) Du, P.; Axe, F. E.; Loew, G. H.; Canuto, S.; Zerner, M. C. *J. Am. Chem. Soc.* **1991**, *113*, 8614–8621.

(15) Schuller, D. J.; Ban, N.; van Huystee, R. B.; McPherson, A.; Poulos, T. L. *Structure* **1996**, *4*, 311–321.

Table 1. Geometries Used for Calculation of Electronic Spectra of Model Heme Peroxidase Complexes


	[L1] [q]		
	(0)	(0)	(-1)
$r(\text{Fe}-\text{O})$, Å	2.03	2.16	1.86
$r(\text{Fe}-\text{N}_\epsilon)$, Å	2.08	2.07	2.07
$r(\text{O}-\text{O})$, Å		1.48	1.30
$r(\text{O}-\text{H})$, Å	0.96	0.96	1.01
$\angle\text{Fe}-\text{O}-\text{O}$, deg		105.9	118
$\angle\text{Fe}-\text{O}-\text{H}$, deg	128.5	151.1	
$\tau\text{H}-\text{O}-\text{O}-\text{H}$, deg		123	
$r\text{Fe}-\text{O}-\text{O}-\text{H}$, deg		72.9	59
$r\text{N}_\epsilon\text{Fe}-\text{O}-\text{O}(\text{H})$, deg		158.3	160
$r(\text{Fe}-\text{N}_{\text{per}})$, Å	2.04	2.04	2.04

Method and Procedures

The optimized geometries of the two model peroxide-peroxidase complexes and the resting state complex chosen for the computations are shown in Table 1. As shown in that table, for all models, the protoporphyrin IX heme unit of CCP was used with all substituents retained. A neutral form of the propionate substituents was used because in the proteins, these substituents interact with polar residues or bound water. An imidazolate (Im⁻) form of the proximal ligand was used because of its proximity to a nearby highly conserved Asp in many peroxidases and the NMR evidence for the transfer of its proton to the Asp.¹⁶ Also, as mentioned above, observed spectral differences between the resting state and compound I forms of peroxidases could only be explained by using an imidazolate form of the proximal ligand.¹³

The initial geometries used for the three species, shown in Table 1, were all based on prior studies. For the resting state, with water as a distal axial ligand, the geometry used was that obtained from energy optimization of the crystal structure of CCP using the AMBER force field.¹⁷ In the neutral HOOH model for the transient peroxide intermediate species, the ligand binding mode and geometry selected for optimization was that obtained from our previous MD simulation of the CCP-HOOH with the peroxide binding to the Fe in a bent end on mode. While no direct structural information yet exists for the Fe-OOH intermediate, the crystal structure of the ferrous-dioxygen bound heme in CCP has been solved.¹⁸ This species differs by a single electron and a proton from the proposed anionic (OOH) intermediate, yet it provides a clue to the dioxy binding orientation and qualitative geometry in the OOH-bound species. The Fe-O distance in this complex is 1.8 Å and the Fe-O1-O2 angle is 133°, quite similar to the geometry in model complexes of dioxygen bound P450's¹⁹ and to a calculated *ab initio* optimized geometry of the dianionic form of this ligand (Loew and Komornicki, unpublished work). In the initial geometry for the

(16) De Ropp, J. S.; Thanabal, V.; La Mar, G. N. *J. Am. Chem. Soc.* **1985**, *107*, 8268-8270.

(17) Cornell, W. D.; Cieplak, P.; Bayly, C. I.; Gould, I. R.; Merz, K. M., Jr.; Fergusson, D. M.; Spellmeyer, D. D.; Fox, T.; Caldwell, J. W.; Kollman, P. A. *J. Am. Chem. Soc.* **1995**, *117*, 5179-5197.

(18) Miller, M. A.; Shaw, A.; Kraut, J. *Nature Struct. Biol.* **1994**, *1*, 524-531.

(19) Schappacher, M.; Richard, L.; Fischer, J.; Weiss, R.; Bill, E.; Montiel-Montoya, R.; Winkler, H.; Trautwein, A. X. *Eur. J. Biochem.* **1987**, *168*, 419-429.

Table 2. Energies^a of the Active MOs in CIS Calculations for Spectra of Model Peroxidase-Peroxide Complexes

[Im ⁻ -Fe-HOOH]		[Im ⁻ -Fe-OOH ⁻]	
Unoccupied MOs			
		5e _{gy}	-0.09
		5e _{gx}	-0.09
		d _{z²}	-0.05
		2b _{1u}	-0.05
2b _{1u}	0.00	d _{x²-y²}	-0.04
4e _{gy}	-0.06	4e _{gy}	0.00
4e _{gx}	-0.06	4e _{gx}	0.00
Occupied MOs			
		1a _{1u}	-0.13
		3a _{2u}	-0.14
		Im-(π)	-0.15
		Im-(π)-3e _g	-0.20
		2b _{2u}	-0.21
		2a _{2u}	-0.21
		Im-(π)-3e _g	-0.22
		2e _g	-0.24
		d _{z²}	-0.24
		d _{xz}	-0.25
		d _{xy}	-0.25
		2e _{gx}	-0.25

^a Energies in hartrees.

anionic OOH⁻ ligand the Fe-O1 and O1-O2 distances and Fe-O1-O2 bond angle were taken from this optimized model compound geometry. All of these species were then optimized using the Amber 4.1 force field to which heme parameters and parameters for the peroxide ligands have been added.

The semiempirical quantum mechanical spin-restricted open-shell (INDO/S-ROHF/CI) method¹²⁻²² was used for all calculations of the electronic structure and spectra of the three complexes with the fixed optimized geometries given in Table 1. This method has been parametrized for transition metals and has been shown to be reliable for calculation of the relative energies of states of different spin multiplicities and for electronic spectra of heme complexes including open-shell species.

Three distinct spin states are possible in Fe³⁺-containing species with a maximum of five unpaired spins: a sextet ($S = 5/2$), a quartet ($S = 3/2$), or a doublet ($S = 1/2$). The ground state multiplet of a given system is determined by factors influencing the iron d-orbital relative energies and the energetics of spin pairing. Calculations of the relative energies of the sextet, quartet, and doublet states of the stable resting state species and the two transient peroxide intermediates allowed the identification of spin state with the lowest energy. This ground state was then used as the reference state for CI calculations in which both the roots of the CI matrix that correspond to frequency and the oscillator strength of each spectral transition were calculated. Each frequency and oscillator strength comprise a spectral line in the calculated spectrum of the modeled peroxidase species.

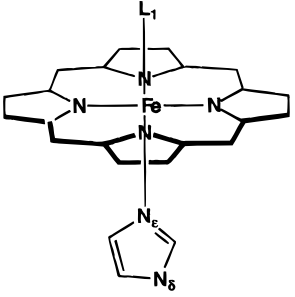
The spectra were calculated using configuration interaction single excitations, with the excitations chosen in accord with the Rumer procedure such that the spin multiplicity of each excited state was taken to be the same as the reference state. The excitation space explored in the CI for all three species considered in this study included the 2e_g, 3e_g, 1a_{1u}, 2a_{2u}, 3a_{2u} porphyrin π orbitals into the unfilled 4e_g(π*) and 2b_{1u}(π*) and iron d-orbitals. In the case of the spectra of the imidazolate-heme with OOH⁻ bound, the excitation space was extended to include the 5e_g(π*) orbital, though it was subsequently determined that excitations involving these latter π* orbitals did not contribute significantly to its spectrum. The energies of significant occupied and empty orbitals used in calculating each spectrum are given in Table 2. The symmetry labels used in this table are for idealized

(20) Ridley, J.; Zerner, M. *Theor. Chim. Acta* **1973**, *32*, 111-134.

(21) Ridley, J. E.; Zerner, M. C. *Theor. Chim. Acta* **1976**, *42*, 223-236.

(22) Edwards, W. D.; Weiner, B.; Zerner, M. C. *J. Am. Chem. Soc.* **1986**, *108*, 2196-2204.

(23) Gouterman, M.; Wagiere, G. H. *J. Mol. Spectrosc.* **1963**, *11*, 108-127.

Table 3. Calculated Relative Energies of Different Spin States and Charge Distribution of Model Ferric Heme Peroxidase Complexes


	L1	H ₂ O	HOOH	OOH ⁻
$E_{5/2}$ (kcal/mol)		0.0	0.0	+8.4
$E_{3/2}$ (kcal/mol)		+13.9	+5.8	+4.9
$E_{1/2}$ (kcal/mol)		+0.20	+4.7	0.0
q_{Fe}		+1.22	1.25	1.13
q_{N_e}		-0.44	-0.44	-0.45
$q_{N_{pyr}}$		-0.48	-0.48	-0.42
q_{O1}		-0.16	-0.23	-0.37
q_{O2}			-0.04	-0.26
q_{L1}		+0.35	+0.31	-0.39
q_{lm}		-0.62	-0.62	-0.67
q_{porp}		-0.95	-1.17	-1.08

D_{4h} symmetry, although these complexes deviate somewhat from this ideal symmetry.

The results of such calculations of such spectra are frequencies, oscillator strengths, and contributions to the intensity from the x , y , and z components of the transition moment. These results have therefore been presented as “delta function” or spectral lines (stick figures) in a frequency/intensity plot in which the position on the x axis indicates the frequency and the height represents its intensity, as well as in tabular form.

In addition we have calculated a simple model convoluted spectra from these “delta function” spectral lines. In this procedure, a Gaussian line shape has been generated whose line width is specified by the user and whose amplitude at the Gaussian center is determined by the oscillator strength of that underlying spectral line. Each spectral line is then expressed as a Gaussian and the contribution of each Gaussian summed into a total spectra. The spectra obtained are based on the simplifying assumption of a uniform line width for each of the underlying transitions and are presented mainly for ease of visualization. The primary data are the spectral line intensities and frequencies but the convoluted band contours are generated in order to make qualitative comparisons with the experimental spectra.

Assignment of each of these spectral lines in terms of the type of excitations contributing to them was also made. These assignments are presented as the contribution of specific molecular orbital excitations to each spectral line. There is no case where a single excitation is responsible for a given spectral line. Each of the calculated frequencies has intensity contributions from many fundamental excitations.

Results and Discussion

Table 3 presents the calculated relative energies and the charge distributions obtained for the three model ferric heme peroxidases complexes in each of the spin states possibly arising from the iron(III) initial $3d^5$ configuration. We see from this table that, for both the resting state species and the hydrogen peroxide (H_2O_2) intermediate, the relative order of spin state energies is $E(^3/2) < E(^1/2) < E(^5/2)$ but with the difference that in the heme resting state species the high- and low-spin states are nearly degenerate. In the peroxyanionic (OOH^-) model of the transient peroxidase intermediate, a low-spin state is the ground state with the spin state energy ordering $E(^1/2) < E(^3/2) < E(^5/2)$, a result typical of ferric heme complexes with anionic ligands.

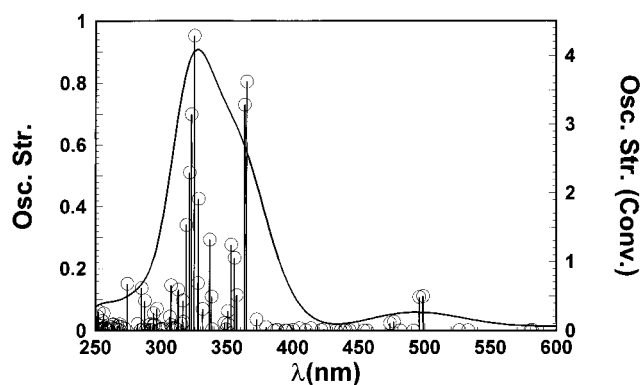


Figure 2. Calculated spectrum of the model resting state of peroxidases. The position of each line is the calculated wavelength. The height of each line is the calculated oscillator strength. Also shown in this figure is the convoluted spectrum calculated from these spectral lines.

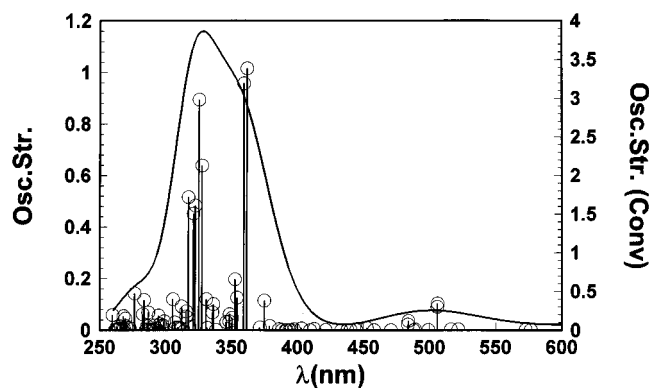


Figure 3. Calculated spectrum of the neutral peroxide form of transient peroxide species of peroxidases. The position of each line is the calculated wavelength. The height of each line is the calculated oscillator strength. Also shown in this figure is the convoluted spectrum calculated from these spectral lines.

The electron distributions in the sextet ground state of both the water and peroxide species are very similar. In both complexes the Fe has a similar positive charge, the ligand's atoms directly bound to it have similar negative charges, the distal ligand has a residual positive charge, and both the imidazolate and porphyrin moieties have significant overall negative charges. Removal of the proton from the neutral HOOH ligand leads to a net gain of $0.7e^-$ on the anionic distal ligand with the remainder of the increase in negative charge on the iron and porphyrin.

The calculated spectrum of the sextet ground state of the peroxide form of the transient species is shown in Figure 2, the calculated spectrum of the sextet ground state of the resting state species in Figure 3, and the calculated spectrum for the doublet ground state of the peroxyanionic species in Figure 4. In these figures each of the spectral lines, corresponding to a given wavelength and oscillator strength (intensity), is plotted. In addition to the spectral line “stick” spectrum, a convoluted spectrum is also presented, in which each of these spectral lines is given an arbitrary line width and then summed to give a total spectrum, as described in the Methods section.

Comparisons of these three calculated spectra with the experimentally observed spectra allow the immediate and striking conclusion that the spectra of the anionic species corresponds to that found for the transient intermediate in one type of rapid scan experiment^{7,8} while that of the neutral HOOH species corresponds to that found for the transient intermediate in the other.¹⁰

As seen in Figures 2 and 3, the calculated spectra of the resting state and the peroxide intermediate are nearly identical,

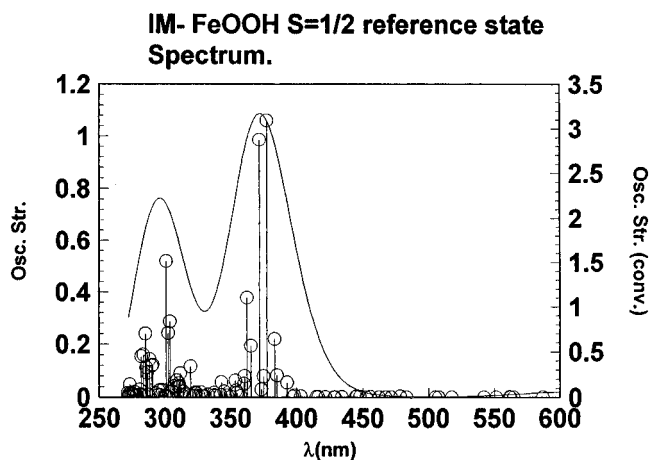


Figure 4. Calculated spectrum of the peroxyanionic form of transient peroxide species of peroxidases. The position of each line is the calculated wavelength. The height of each line is the calculated oscillator strength. Also shown in this figure is the convoluted spectrum calculated from these spectral lines.

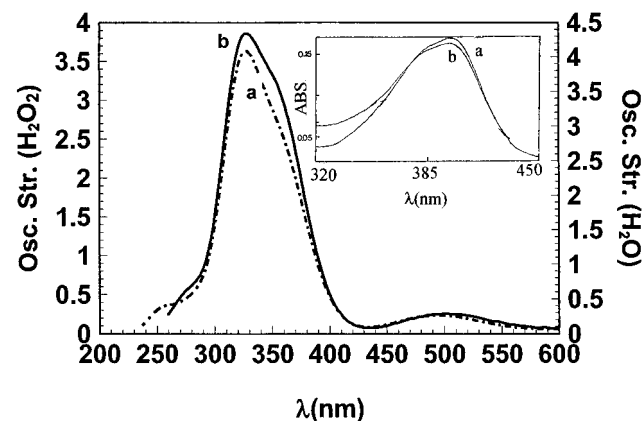


Figure 5. Superposition of the calculated resting state and neutral peroxide form of transient peroxide species of peroxidases. Shown in the insert is the observed resting state and transient species spectra of the R38L mutant HRP-C.¹⁰

a result observed in the studies of the reaction of peroxide with the mutant R38L HRP. This striking similarity between calculated and observed spectra is clearly seen in Figure 5, which shows both the calculated spectra of the resting state and the neutral peroxide species and, as an insert, the observed spectra of the resting state and the transient species seen with the R38L HRP experiment. Comparisons of the calculated and observed spectra provide strong evidence that the neutral peroxide complex is the transient species observed in these experiments.

In marked contrast, comparing Figures 2 and 4, the calculated spectra of the peroxyanion species has the extra shorter wavelength intense band associated with the intermediate created prior to compound I formation in the reaction of peroxide with WT HRP and with a soluble model of HRP. Shown in Figure 6 are the calculated spectra of both the resting state and the peroxyanionic species and, as an insert, the observed spectra for the resting state and transient species in those experiments. While the INDO/S spectra uniformly differ by a ca. 30-nm shift from the experimental spectra, the significant result is that both calculated and observed spectra of the transient species have two similar high-intensity bands, the one observed in the resting state and a new one at shorter wavelengths. Thus, good agreement has been obtained between the calculated and observed differences in the transient and resting state species. Based on the finding of this similarity, the presence of an unusual hyperporphyrin split Soret in both the calculated and

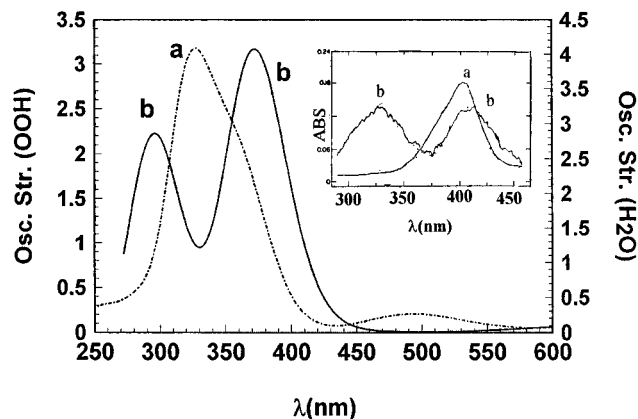


Figure 6. Superposition of the calculated resting state and peroxyanion form of transient peroxide species of peroxidases. Shown in the insert is the observed resting state and transient species spectra of the wt HRP-C.⁷

observed transient spectra that is absent in the resting state spectra, we propose that the peroxyanionic form of the peroxidase-peroxide intermediate is the transient species responsible for this observed spectra.

Having used the calculated spectra to identify the species associated with the transient spectra observed, we turn now to the assignment of these spectra. As seen in Figures 2–4, the high-intensity bands in the 250–450 nm wavelength region are composed of many individual spectral lines of varying intensity. Each of these individual spectral lines is in turn composed of contributions from many different orbital excitations. Given in Tables 4 and 5 is an assignment of each of the spectral lines for both types of peroxide intermediates in terms of the percent contribution from the major excitations, together with their calculated frequencies (wavenumbers), wavelengths, and oscillator strengths. We see from these tables that no spectral line is due to a single excitation.

The history of the investigation of the origin of the electronic spectra of heme complexes is a long one, dating back to the pioneering work of Gouterman.²³ These investigators postulated that excitations in a four-orbital model, from the occupied porphyrin a_{1u} and a_{2u} π orbitals to the lowest unoccupied $e_g(\pi^*)$ (see Table 2), could completely explain the two features common to all heme spectra: the weak bands in the visible region of 500–600 nm, the Q bands, and the intense band in the 400-nm region, the Soret or B band. Using the more accurate and reliable INDO-S/ROHF/CI method now available for these spectral calculations, the much more complex assignments obtained here have been found to be typical of all the heme spectra we have thus far calculated. For historical reasons, however, we have maintained the labels Q and B for spectral transitions that have a significant contribution from excitations from $1a_{1u}$ and $3a_{2u}$ π orbitals to the $4e_g(\pi^*)$ orbitals. The additional bands observed are labeled by their most prominent contributions.

Table 4 gives the assignment of the individual spectral lines for the peroxide species. Each of the lines contributing to the B band intensity contain varying amounts of the traditional $1a_{1u}$, $3a_{2u}$ to $4e_g(\pi^*)$ excitations that give this band its name. The lines of maximum intensity at 360 nm have nearly 50% of this excitation character, while the lower intensity lines have admixtures of other porphyrin $\pi \rightarrow \pi^*$ transitions as well as iron-d-orbital to porphyrin π^* (charge transfer) and imidazolate to porphyrin excitations. The Q band is composed more completely of the traditional four-orbital excitations, but also has some charge transfer component. Since these full protoporphyrin IX model peroxidase complexes optimized from an

Table 4. Calculated Spectra for the Peroxide–Peroxidase Complex [Im–Fe–HOOH]

ν (cm ⁻¹)	λ (nm)	f	label	main excitations	
				excitations	%
14941	669	0.05	Q	3a _{2u} → 4e _g	52
				1a _{1u} → 4e _g	38
				1a _{1u} → d _{yz}	5
14988	667	0.05	Q	1a _{1u} → 4e _g	53
				3a _{2u} → 4e _g	14
				Im-(π)-3e _g → 2b _{1u}	27
19760	506	0.102	CT	3a _{2u} → d _{yz}	29
				1a _{1u} → d _{xz}	17
				1a _{1u} → d _{yz}	12
				Im-(π)-3e _g → 2b _{1u}	10
26688	374	0.114	CT	1a _{1u} → 4e _g	13
				Im-(π)-3e _g → d _{z²}	52
				Im-(π)-3e _g → 4e _g	6
				3a _{2u} → 4e _g	5
27665	360 (400) ^a	1.0	B	1a _{1u} → 4e _g	21
				3a _{2u} → 4e _g	19
				2a _{2u} → 4e _g	13
				Im-(π) → 2b _{1u}	13
				2b _{2u} → 2b _{1u}	13
27847	359	0.96	B	3a _{2u} → 4e _g	32
				1a _{2u} → 4e _g	14
				2a _{2u} → 4e _g	22
28243	354	0.13	B	3a _{2u} → 4e _g	78
				28368	352
				1a _{1u} → 4e _g	
				2a _{2u} → 4e _g	10
				d _{z²} → 4e _g	6
30236	330	0.12	B	1a _{1u} → 4e _g	30
				1a _{1u} → 2b _{1u}	30
				Im-(π) → 4e _g	7
30549	327	0.64	B	3a _{2u} → 4e _g	22
				1a _{2u} → 4e _g	12
				2b _{2u} → 2b _{1u}	16
				1a _{1u} → 2b _{1u}	9
30768	325	0.89	B	2a _{2u} → 4e _g	28
				3a _{2u} → 4e _g	19
				1a _{1u} → 2b _{1u}	14
				2b _{2u} → 4e _g	13
30103	330	0.48	B	3a _{2u} → 4e _g	14
				2a _{2u} → 4e _g	11
				Im-(π)-3e _g → d _{yz}	13
				3e _g → 4e _g	14
31164	320	0.45	B	1a _{1u} → 4e _g	5
				Im-(π) → 2b _{1u}	21
				Im-(π)-3e _g → 4e _g	13
				2a _{2u} → 4e _g	5
31533	317	0.52	B	1a _{1u} → 4e _g	5
				3e _g → 4e _g	23
				1a _{1u} → 4e _g	19
				3a _{2u} → 4e _g	8

^a Experimental value in ref 10.

crystal structure of CCP have significant deviations from the ideal D_{4h} symmetry of the porphine ring itself, these mixtures of contributing excitations are to be expected.

The complexity of the Soret band for both the resting state and neutral peroxide intermediate is shown in Table 6, where the frequency and oscillator strengths of all the B-band lines are given side by side. Given this complexity, the similarity found between the calculated spectrum of the resting state and the peroxide intermediate is striking and parallels the behavior in the observed spectra of the reaction between peroxide and R38L HRP-C (Figure 5).

Given in Table 5 is the assignment of the calculated spectrum of the peroxyanionic form of the transient peroxide complex in its doublet ground state. We see that the two intense bands, labeled B and B', both include several individual lines with varying amounts of the traditional four-orbital (3a_{2u}(π), 1a_{1u}(π), and 4e_g(π^*)) excitations although the composition of these bands

Table 5. Calculated Spectra for the Peroxide-Peroxidase Complex [Im-Fe-OOH-]

ν (cm ⁻¹)	λ (nm)	f	label	main excitations	
				excitations	%
15905	629	0.04	Q	1a _{1u} → 4e _g	55
				3a _{2u} → 4e _g	42
				1a _{1u} → 4e _g	51
15987	626	0.03	Q	3a _{2u} → 4e _g	46
				Im-(π) → 4e _g	16
				d _{xz} → 4e _g	15
26084	383	0.22	B(CT)	3a _{2u} → 4e _g	10
				1a _{1u} → 4e _g	10
				1a _{1u} → 4e _g	30
				3a _{2u} → 4e _g	18
26486	378 (400) ^a	1.06	B	3a _{2u} → 4e _g	29
				1a _{1u} → 4e _g	26
				Im-(π) → 4e _g	11
26892	372	0.99	B	d _{yz} → 4e _g	9
				2b _{2u} → 4e _g	29
				Im-(π)-3e _g → 4e _g	13
				3a _{2u} → 4e _g	7
32913	304	0.29	B'	d _{yz} → 4e _g	7
				1a _{1u} → 4e _g	2
				Im-(π)-3e _g → 4e _g	37
				Im-(π) → 4e _g	12
33067	302	0.24	B'	Im-(π) → 4e _g	8
				2b _{2u} → 4e _g	26
				2a _{2u} → 4e _g	13
				3a _{2u} → 2b _{1u}	13
33233	300 (330) ^a	0.52	B'	Im-(π)-3e _g → 4e _g	9
				3a _{2u} → 4e _g	4
				2a _{2u} → 4e _g	32
				Im-(π) → 2b _{1u}	42
35063	250	0.24	B'	2a _{2u} → 4e _g	32
				Im-(π) → 2b _{1u}	42
				Im-(π) → 2b _{1u}	42

^a Experimental value in ref 7.

is multifaceted. Table 6 compares the B and B' components of the peroxyanionic form of the transient peroxide complex side by side with the resting state B band.

It is challenging to understand the origin of the split Soret found in the anionic form of the peroxide intermediate, whether it is the same as in the P450s, and why it is absent in the neutral form of the peroxide intermediate. The prosthetic groups of peroxidases, globins, and P450s are identical protoporphyrin IX heme complexes except for the proximal axial ligand, which is a mercaptide from a nearby conserved cysteine residue in the P450s instead of the imidazole ligand typical of peroxidases and globins. Yet, the ferrous carbonyl complex of both the globins and the peroxidases exhibits a normal Soret at 420 nm while that of the P450s exhibits a hyperporphyrin spectra with one intense peak at 450 nm and the other at 368 nm.

In a previous study made using the same INDO/SCF/CI method employed here, we calculated the spectra of a model ferrous P450 carbonyl complex and a model peroxidase/myoglobin complex in the ferrous carbonyl form with only a difference in the proximal axial.^{24,25} In agreement with observation, the calculated spectra of the peroxidase complex resulted in a normal single intense Soret, while that of the P450 complex was found to be a split Soret with one band to the red and the other to the blue of the peroxidase Soret band. From this and subsequent spectral calculations of other P450 complexes that exhibit the split pattern,^{25–27} the origin of this splitting could be clearly identified. It is caused by a mixing

(24) Loew, G. H.; Rohmer, M. M. *J. Am. Chem. Soc.* **1980**, *102*, 3655–3657.(25) Loew, G. H.; Herman, Z. S.; Rohmer, M. M.; Goldblum, A.; Pudzianowski, A. In *Quantum Chemistry in Biomedical Sciences*; Weinstein, H., Green, J. P., Eds. *Ann. N.Y. Acad. Sci.* **1981**, *367*, 192–218.(26) Loew, G. H.; Goldblum, A. *J. Am. Chem. Soc.* **1980**, *102*, 3657–3659.(27) Waleh, A.; Collins, J.; Loew, G. H.; Zerner, M. C. *Int. J. Quantum Chem.: Quantum Biol. Symp.* **1986**, *29*, 1575–1589.

Table 6. Comparison of Calculated Spectra in the Soret Region of Model Peroxidase in the Resting State and Peroxide Complexes

	(Fe-H ₂ O)		Fe-HOOH (<i>S</i> = 5/2)		Fe(OOH) (<i>S</i> = 1/2)			
Q	668 (0.05)		668 (0.05)		629 (0.04)			
	665 (0.04)		667 (0.04)		626 (0.03)			
B	365 (0.80)	<u>400^{a,b}</u>	B	361 (1.01)	400 ^a	B	378 (1.06)	<u>400^b</u>
	363 (0.73)			359 (0.96)			372 (0.99)	
	328 (0.42)			327 (0.64)			362 (0.38)	
	327 (0.95)			325 (0.89)				
	323 (0.70)			322 (0.48)				
	321 (0.51)			321 (0.45)		B'	304 (0.29)	<u>330^b</u>
	319 (0.34)			317 (0.52)			301 (0.24)	
							301 (0.52)	
							291 (0.12)	

^a Experimental value in ref 10. ^b Experimental value in ref 7.

of the unpaired orbitals of the sulfur ligands with the 3a_{2u} π orbital of the porphyrin. This mixing affected the relative energies of the 1a_{1u} and 3a_{2u} π orbitals, leading to the split Soret pattern. No such mixing and no such splitting were observed between the imidazole ligand and the porphyrin π orbitals of the model ferrous peroxidase carbonyl complex model.

Looking at the molecular orbital composition of the filled and empty orbitals used to calculate the spectra for the transient ferric peroxidase peroxyanion intermediate, we see that, in common with the ferrous peroxidase carbonyl complex, there is no mixing of the imidazole orbitals with either the 1a_{1u} or the 3a_{2u} porphyrin π orbital (Table 2). Thus the origin of the split Soret is not the same as in the P450s. What then is the origin of the hyperporphyrin pattern seen for this transient peroxyanion intermediate and why is it absent in the peroxide intermediate?

As seen in Table 2, there is a mixing of two occupied orbitals of 3e_g π orbitals with the imidazole π orbitals. We further note in Table 5 that excitations from these filled orbitals to the 4e_g(π^*) orbital make a significant contribution to the new higher energy B' band of the peroxyanion species. Although, as seen in Table 2, these orbitals are also present in the neutral peroxide species, they do not make a significant contribution to any of the spectral transitions, resulting in a normal B band (Table 4). The diminished contribution of the transition from the Im-(π)-3e_g(π) mixed orbital to the lowest empty 4e_g(π^*) in this species could be due to the greatly increased energy

separation between them. Thus it seems that the presence of the Im-(π)-3e_g(π) mixing in filled orbitals and the relative energy of these orbitals with respect to the lowest empty 4e_g(π^*) orbitals are the factors contributing to a hyperporphyrin spectra in the anionic form and its absence in the neutral form of the transient peroxide intermediate of peroxidases.

The identification of a peroxyanionic form with the transient peroxide species in the wt HRP and of a neutral form of this species in the R38L mutant HRP, with a slower rate of compound I formation, has important mechanistic implications. Both the distal histidine and the arginine that was mutated have been shown to play key roles in compound I formation from the peroxide intermediate. The trapping of the neutral peroxide species in the mutant and the peroxyanion form in the WT implies that the slower rate of compound I formation in the mutant is due to the interference with proton transfer from the peroxide to the imidazole, and provides additional evidence that this process is important in the rapid formation of compound I. Thus the results obtained provide additional insight into the important rate-determining steps in compound I formation in peroxidases and the interactive roles of the distal arginine and histidine residues in this process.

Acknowledgment. Support for this work from NSF grant MCB-9305619 is gratefully acknowledged.

JA9617247